Japan) and then were incubated with antibodies directed against Cx43 (1:1000) and β-actin (1:1000) as the primary antibody overnight at 4 °C. After repeated rinsing in PBS–Tween, the immunoblots were incubated with a peroxidase-conjugated antibody against rabbit (1:5000) at room temperature for 1 h. Membranes were developed by enhanced chemiluminescence according to the manufacturer's instructions (Amersham Pharmacia Biotech).

3. Results

3.1. Cell viability

In order to evaluate the affect of HMW HA on cell viability, HIT-T15 cells were incubated with HA-coated (0.01, 0.05, 0.1, 0.5, and 1.0 mg/dish) or -added (0.01, 0.05, 0.1, 0.5, and 1.0 mg/ml) for 24 h. After 24 h exposure to HA-added, there was no significant change in the viable HIT-T15 cell number at the low concentration of HA-added (⩽1.0 mg/dish) compared to control. In contrast, after 24 h of incubation, the cell viability of HIT-T15 cells grown on high concentration HA-coated dishes (⩾1.0 mg/dish) was significantly less than on low concentration HA-coated and control (Fig. 1). Therefore, all further studies were conducted using low concentration of HA (⩽0.5 mg/dish).

3.2. Insulin secretion and insulin content

HIT-T15 cells, retain glucose-stimulated insulin secretion, showed an increase in insulin secretion as a function of stimulation. Thus, their insulin output was 2.73±0.36 and 3.90±0.41 pg/μg protein in the base and glucose-stimulation (11.1 mM), respectively ($n = 9$ dishes from three independent experiments). When these cells were exposed to a low concentration of HA-coating (0.1, 0.25, and 0.5 mg/dish) for 24 h, their insulin secretion was significantly increased in the presence of glucose-stimulation (Fig. 2). However, in contrast, when HIT-T15 cells were incubated with HA-addition for 24 h, the increasing effect was not exhibited. The insulin secretion was without a difference between control and HA-addition (Fig. 2). On the other hand, after acid-ethanol extraction, we found that the insulin content of the HIT-T15 cells grown onto the HA-coated dishes was significantly increased but not HA-added (Fig. 3).

GJIC and Cx43 are thought to be crucial regulatory mechanisms of insulin secretion and insulin content. As described above, HA-coating increased insulin secretion and insulin content of the HIT-T15 cells. In addition, Park and Tsuchiya [6] reported that HMW HA-coating can enhance the function of GJIC in normal human dermal fibroblasts but not HA-addition. Hence, all further studies on the mechanism of insulin secretion and insulin content were conducted using HA-coating.

3.3. Dye transfer

We assessed the function of GJIC using Lucifer yellow by counting the number of dye-transferred cells at 2 min

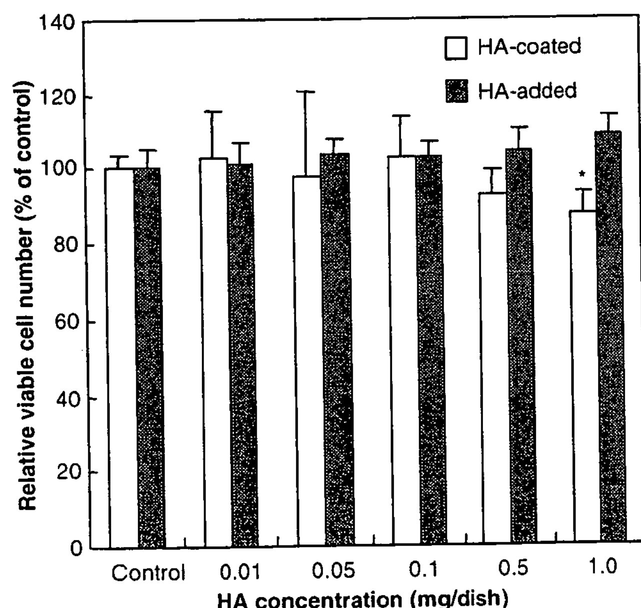

Fig. 1. Concentration-dependent effects of HA-treatment on viability of HIT-T15 cell. After HIT-T15 cells were incubated with HA-coated or HA-added for 24 h, the viable cell numbers of HIT-T15 cell were determined by WST-8 assay as described in methods. Each value denotes the mean±S.D. of three separate experiments. *$P \leqslant 0.05$ compared to control under the HA-coated condition.

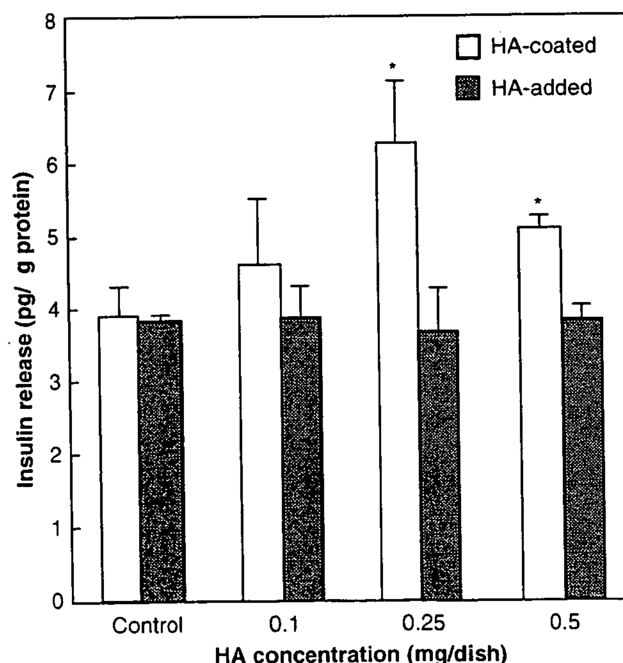

Fig. 2. Insulin secretion from HIT-T15 cells by HA-treatment. HIT-T15 cells were incubated with HA-coating (□) or HA-added (■) for 24 h and then stimulated for 60 min with 11.1 mM glucose in KRB buffer. The released insulin in the spent medium was determined by ELISA insulin kit. Each value denotes the mean±S.D. of three separate experiments. *$P \leqslant 0.05$, compared to control in the presence of glucose.

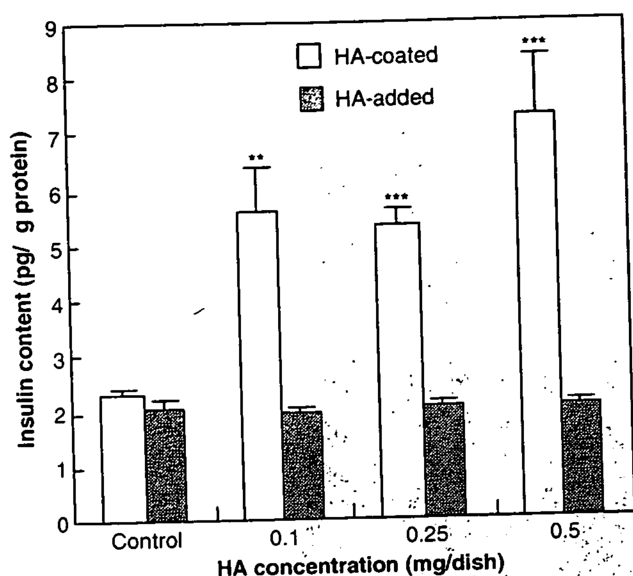

Fig. 3. Insulin content of HIT-T15 cells incubated with HA-coated (□), and HA-added (■). Cells were incubated in the presence of different HA concentrations (0.1–0.5 mg/dish) for 24 h and then stimulated for 60 min with 11.1 mM glucose. The insulin content in the extracts was determined by ELISA insulin kit. Each value denotes the mean ± S.D. of three separate experiments. ** $P \leq 0.01$ and *** $P \leq 0.001$ compared to control.

after microinjection. Fig. 4A shows the patterns of dye transfer in HIT-T15 cells treated with HA-coating (0.1, 0.25, and 0.5 mg/dish) for 24 h. Most microinjections led to the intercellular transfer of Lucifer yellow, indicating the frequent coupling of HIT-T15 cells. Under control conditions, microinjection experiments revealed that 47.1% of HIT-T15 cells transferred Lucifer yellow with a limited number (1.5 ± 0.6) of microinjection cells. In HA-coated conditions, almost injected cells (95%) showed Lucifer yellow dye transfer, the number of Lucifer yellow-transferred cells (3.2 ± 1.3, 4.4 ± 1.9, and 4.1 ± 1.9, respectively) was more than that of the control condition ($P < 0.001$) (Fig. 4B), which indicated that GJIC function was activated by the HA-coating.

3.4. Cx43 expression

Cx43 is the 43-kDa member of a conserved family of membrane spanning gap-junction proteins. To provide further evidence that the HA-coating increased the function of GJIC, relative to the levels of actin, comparable levels of immunolabeled Cx43 was detected in 0.1, 0.25, and 0.5 mg/dish of HA-coating cells. Whole cell lysates from HA-coated dish were subjected to SDS–PAGE. Immunoblot analysis was performed with an antibody that specifically recognized Cx43 or β-actin. A Western blot analysis revealed that Cx43 proteins are present in cultured HIT-T15 cells in three forms at 43 kDa region, consisting of a nonphosphorylated form and phosphorylated forms (P1 and P2). HA-coating appeared to induce a greater concentration-dependent increase in all three Cx43 protein levels than control. However, the protein level of β-actin was no different from them (Fig. 5), indicating HA-coating increases the function of GJIC via the expression of Cx43. To account for differences in loading, proteins were both stained with Coomassie blue and immunolabeled for β-actin. The latter staining, which did not change in our experiments relative to that of Coomassie blue (data not shown), was used as an internal standard. These results suggested that HA-coating specifically increased the Cx43 protein but not all cell proteins of HIT-T15 cells.

4. Discussion

The transplantation strategy of bioartificial pancreas is to construct bioartificial tissues in vitro from cells or islets and a support matrix and implant the construct into the body in place of the original. The support matrix must be able to maintain the functions of differentiated cells or contain and/or be able to release appropriate biological signaling information to promote and maintain cell adhesion and differentiation. HA is a high-molecular-mass polysaccharide of support matrix in the body, which is believed to play roles in maintaining various physiological functions including water and plasma protein homeostasis, cell proliferation, cell locomotion, and migration [3]. HA is plentiful, easy to extract and mold into a variety of shape, and biodegradable. It is thus widely used matrix biomaterial for bioartificial tissues [10]. In this study, we investigated whether administration of various concentration of HMW HA influences the viability, GJIC, and insulin secretion of pancreatic β-cells as a matrix biomaterial of bioartificial pancreatic constructs.

Previous study has shown that HMW (310 and 800 kDa) HA-coating (2.0 mg/dish) resulted in low adhesiveness to the cells and the decrease of viability in normal human dermal fibroblasts, because of the change in GJIC functions and induction of various genes including cytokines, adhesion molecules, and growth factors [6,11,12]. In the present study, similar results were obtained. After 12 h, the HIT-T15 cells grown into low concentration HA-coated dishes (0.1, 0.25, and 0.5 mg/dish) and control cells already had attached and confluent but not high concentration HA-coated dishes (≥1.0 mg/dish). We showed that treatment with high concentration of HMW (1680 kDa) HA-coated dose dependently inhibited the viability of HIT-T15 cells. In contrast, there was no difference in viability of HIT-T15 cells between the control and HA-added dishes. These results indicated that among the individual qualities of ECM, the viscosity plays a decisive role. The changes of cell viability by HA-treatment may depend on the cell attachment activity. The difference in cell attachment activity may depend on the surface structure of the coated HA, because the HMW HA-coated surface provides a stable anionic surface that prevents cells attachment at the early time [13]. This result suggests that the molecular-weight size of HA and its

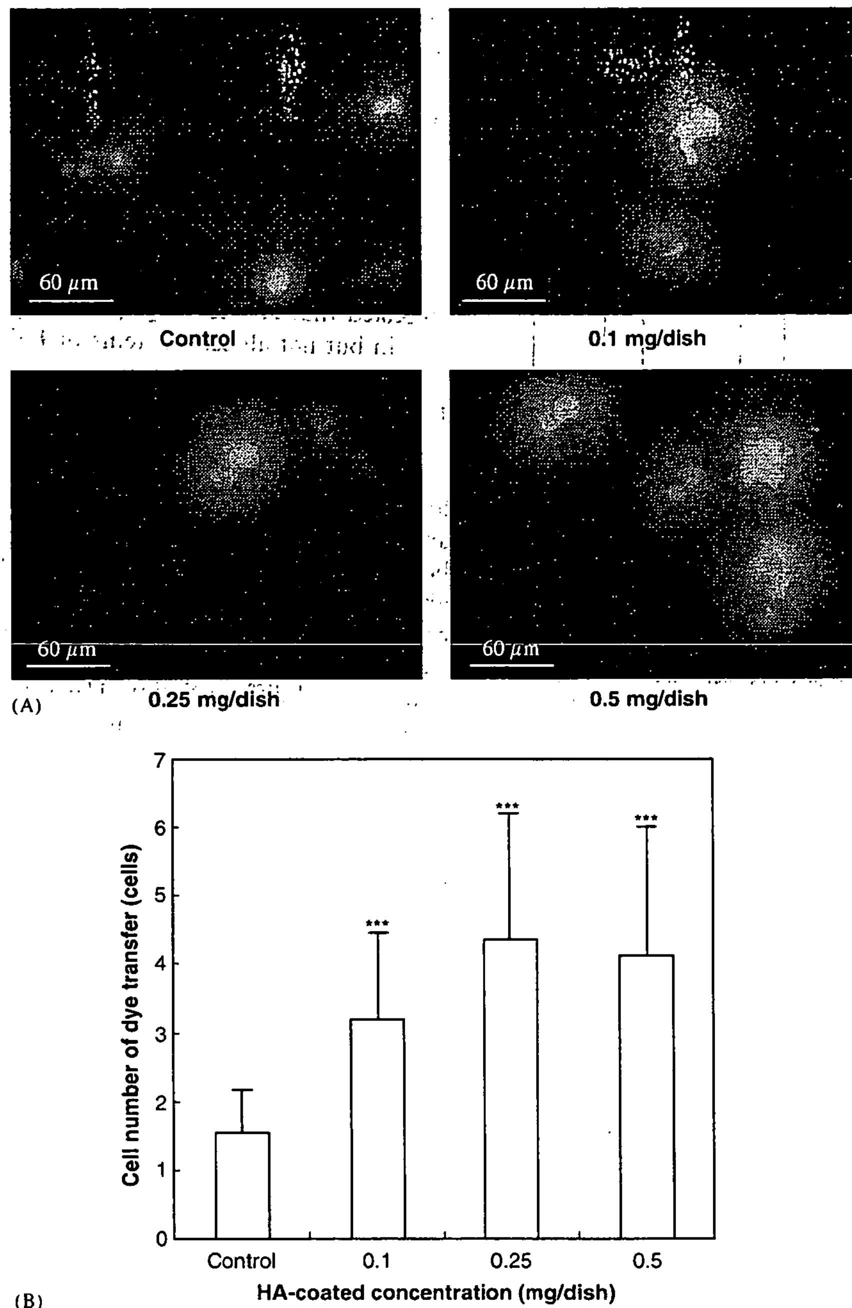

Fig. 4. Concentration-dependent effects of HA-coating on dye transfer in HIT-T15 cells. Cell adherent to glass coverslips were microinjected with 4% Lucifer yellow. Transfer of dye to neighboring cells was assessed by epifluorescence microscopy 2 min later. This is a representative expression of 18 injections per group (A). The number of neighboring cells that received dye was quantified (B). Each value expressed as the mean ± S.D. ($n = 18$). *** $P \leqslant 0.001$ compared to control.

application method and concentration are important factors for generating biocompatible tissue-engineered products.

It has been reported that single β-cells (which cannot form gap junctions) show alterations in both basal and stimulated release of insulin, in protein biosynthesis, and in the expression of the insulin gene. The sustained stimulation of insulin release is associated with an increase in β-cells coupling, in the expression of gap junctions by a unique mechanism for direct equilibration of ionic and molecular gradients between nearby cells [14–16]. In this study, we found that the insulin release and insulin content are increased and GJIC activity was enhanced in cultured HIT-T15 cells by low concentration HMW HA-coating in spite of the inhibitory effects on the cell viability in high concentration HA-coating dishes. This finding was consistent with previous reports. The effect of HA may be influenced by the viscosity of HA, the concentration of

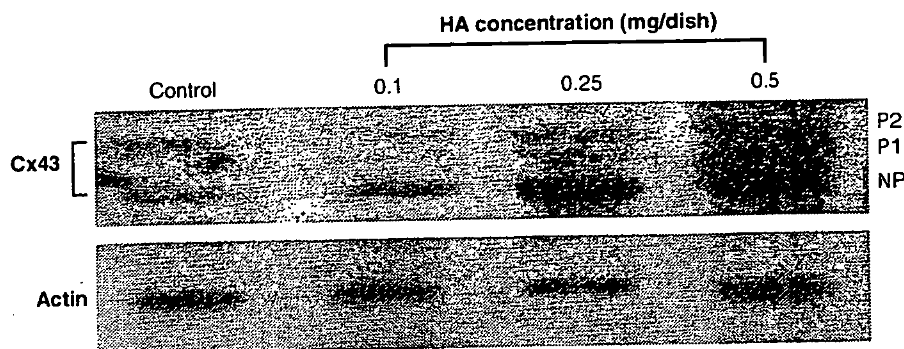

Fig. 5. Identification of Cx43 in HIT-T15 cells grown on the HA-coating dish by Western blot analysis. After HIT-T15 cells were incubated into HA-coated dish for 24 h, cells were lysed and proteins (20 μg) were separated by SDS–PAGE followed by Western blotting using rabbit anti-Cx43 antibody. Actin immunostaining was used to assess equivalent protein loading. This is a representative autoradiogram of three experiments.

FBS and the nutrients in media such as hormone, growth factor (FGF, etc.), cell adhesion molecule (N-CAM and cadherins), and transportation protein [6,17]. As a result, the HIT-T15 cells can use these nutrients and the nutrient-enriched substrata (e.g. natural ECMs) by ionic interaction and the binding of HMW HA to various kinds of cytokines, to change the cell aggregations, resulting in the increase of GJIC. With the evidence above, the enhancement of GJIC activity induced by HA-coating participated in the regulation of insulin release and insulin biosynthesis. On the other hand, the glucose stimulus-secretion coupling in β-cells generated several signals, including a signal to secrete preformed insulin stored in secretory vesicles, a signal, which may be the same or different, to secrete newly made insulin, and a signal to synthesize more insulin. The mechanism of glucose-induced insulin secretion is distinct from that of glucose-induced proinsulin biosynthesis and insulin gene transcription [18]. Moreover, the qualities of ECM affect the insulin release [19]. Therefore, it is possible that HA-coated dishes promoted a large increase in insulin synthesis but only a modest increase in insulin release. The detailed action mechanism should be investigated in the next study.

In native and tumoral insulin-producing pancreatic β-cells, gap-junction protein Cx43 has been identified. Furthermore, the stable transfection of the gene coding for Cx43 induces the expression of functional gap-junction channels and improves both the biosynthetic and secretory defects of the cells. Cx43-transfection and incidence of junctional coupling also secrete more insulin than wild-type and noncommunicating cells, the absence of Cx43 implicated in the loss of β-cell-specific functions in vitro and in vivo [9,14]. In this study, HA-coating expressing high levels of the Cx43, gap junctions, and coupling, showed the striking enhancement of the amounts of stored hormone in HIT-T15 cells and promoted the glucose-induced insulin release, indicating that adequate levels of Cx43 and coupling are required for proper insulin production. These results provide further evidence that HA-coating increases the pancreatic β-cells function by enhancing the function of Cx43-mediated GJIC.

5. Conclusion

In conclusion, the function of GJIC is considered to be a useful marker for evaluating tissue-engineered products. The data obtained in this study show that gap junctions contribute to regulating some still-unknown mechanism to couple the stimulus-secretion of HIT-T15 cells under the condition of low concentration HA-coating. The growth regulation with a bioartificial pancreatic construct using HA is achievable. These results give useful information on design biocompatibility of HA when the HA is used as a biomaterial for bioartificial pancreas. HA-coating may be a new technique for constructing three-dimensional bioartificial pancreas in tissue engineering.

Acknowledgements

This work was supported in part by a Grant-in-Aid for Scientific Research on Advanced Medical Technology from Ministry of Health, Labour and Welfare, Japan and a Grant-in-Aid from Japan Human Sciences Foundations.

References

[1] Soon-Shiong P, Heintz R, Yao Q, Yao Z, Zheng T, Murphy M, et al. Insulin independence in a type 1 diabetic patient after encapsulated islet transplantation. Lancet 1994;343:950–1.

[2] Maki T, Monaco AP, Mullon CJP, Solomon BA. Early treatment of diabetes with porcine islets in a bioartificial pancreas. Tissue Eng 1996;2:299–306.

[3] Laurent TC, Fraser JR. Hyaluronan. FASEB J 1992;6(7):2397–404.

[4] Knudson CB, Knudson W. Hyaluronan-binding proteins in development, tissue homeostasis, and disease. FASEB J 1993;7(13):1233–41.

[5] Nagy JI, Hossain MZ, Lynn BD, Curpen GE, Yang S, Turley EA. Increased connexin-43 and gap junctional communication correlates with altered phenotypic characteristics of cells overexpressing the receptor for hyaluronic acid-mediated motility. Cell Growth Differ 1996;7(6):745–51.

[6] Park JU, Tsuchiya T. Increase in gap-junctional intercellular communications (GJIC) of normal human dermal fibroblasts

(NHDF) on surfaces coated with high-molecular-weight hyaluronic acid (HMW HA). Inc J Biomed Mater Res 2002;60(4):541–7.
[7] Meda P. The role of gap junction membrane channels in secretion and hormonal action. J Bioenergy Biomembr 1996;28(4): 369–77.
[8] Meda P, Bosco D, Chanson M, Giordano E, Vallar L, Wollheim C, et al. Rapid and reversible secretion changes during uncoupling of rat insulin-producing cells. J Clin Invest 1990;86(3): 759–68.
[9] Vozzi C, Ullrich S, Charollais A, Philippe J, Qeci L, Medz P. Adequate connexin-mediated coupling is required for proper insulin production. J Cell Biol 1995;131(6 Part 1):1561–72.
[10] Hubbell JA. Materials as morphogenetic guides in tissue engineering. Curr Opin Biotechnol 2003;14(5):551–8.
[11] Park JU, Tsuchiya T. Increase in gap junctional intercellular communications by high molecular weight hyaluronic acid associated with fibroblast growth factor 2 and keratinocyte growth factor production in normal human dermal fibroblasts. Tissue Eng 2002;8(3):419–27.
[12] Nakamura K, Yokohama S, Yoneda M, Okamoto S, Tamaki Y, Ito T, et al. High, but not low, molecular weight hyaluronan prevents T-cell-mediated liver injury by reducing proinflammatory cytokines in mice. J Gastroenterol 2004;39(4):346–54.
[13] Forrester JV, Balazs EA. Inhibition of phagocytosis by high molecular weight hyaluronate. Immunology 1980;40(3):435–46.
[14] Meda P, Chanson M, Pepper M. In vivo modulation of connexin-43 gene expression and junctional coupling of pancreatic β-cells. Exp Cell Res 1991;192(2):469–80.
[15] Charollais A, Gjinovci A, Huarte J, Bauquis J, Nadal A, Martin F, et al. Junctional communication of pancreatic beta cells contributes to control of insulin secretion and glucose tolerance. J Clin Invest 2000;106:235–43.
[16] Meda P, Pepper MS, Traub O. Differential expression of gap junction connexins in endocrine and exocrine glands. Endocrinology 1993: 133(5):2371–8.
[17] Charollais A, Serre V, Mock C, Cogne F, Bosco D, Meda P. Loss of α_1 connexin does not alter the prenatal differentiation of pancreatic β-cells and leads to the identification of another islet cell connexin. Dev Genet 1999;24(1–2):13–26.
[18] Barton W, Cristina A, Isabelle B, Melissa KL, Christopher JR. Glucose-induced translational control of proinsulin biosynthesis is proportional to preproinsulin mRNA levels in islet β-cells but not regulated via a positive feedback of secreted insulin. J Biol Chem 2003;278(43):42080–90.
[19] Lim F, Sun AM. Microencapsulated islets as bioartificial endocrine pancreas. Science 1980;210:908–10.

WILEY InterScience® DISCOVER SOMETHING GREAT

A mouse strain difference in tumorigenesis induced by biodegradable polymers

Saifuddin Ahmed, Toshie Tsuchiya
Division of Medical Devices, National Institute of Health Sciences, 1–18-1 Kamiyoga, Setagaya-ku, Tokyo 158-8501, Japan

Received 13 November 2005; accepted 6 February 2006
Published online 10 August 2006 in Wiley InterScience (www.interscience.wiley.com). DOI: 10.1002/jbm.a.30753

Abstract: The use of poly-L-lactic acid (PLLA) surgical implants for repair of bone fractures has gained popularity in the past decade. The aim of this study was to evaluate the *in vivo* effect of PLLA plates on subcutaneous tissue in two mouse strains, BALB/cJ and SJL/J, which have higher and lower tumorigenicity, respectively. Gap-junctional intercellular communication and protein expression of connexin 43 were significantly suppressed, whereas secretion of transforming growth factor-β1 and expression of extracellular matrix, insulin-like growth factor binding protein 3, and cysteine-rich intestinal protein 2 were significantly increased in PLLA-implanted BALB/cJ mice when compared with BALB/cJ controls. Finally, tumors were formed after implantation of cultured cells from the more-tumorigenic BALB/cJ, but not SJL/J, mice into nude mice. © 2006 Wiley Periodicals, Inc. J Biomed Mater Res 79A: 409–417, 2006

Key words: poly-L-lactic acid; gap-junctional intercellular communication; transforming growth factor-β1; connexin 43; nude mice

INTRODUCTION

The morphologic, chemical, and surface electrical characteristics of a biomaterial can influence the extent of the cellular response to an implant,[1,2] but host factors also contribute, so that an identical material implanted in different species[3,4] or at different anatomical locations[5,6] may elicit different degrees of response. Poly-L-lactic acid (PLLA) is a synthetic degradable polymer with good biocompatibility that is widely used clinically for surgical implants and as a bioabsorbable suture material.[7,8] Long-term implants of PLLA produced tumors in rats,[9] and adverse effects were also reported in other animal experiments.[10] All tumors are generally viewed as the result of disruption of the homeostatic regulation of the cell's ability to respond to extracellular signals, which triggers intracellular signal transduction abnormalities.[11] During the transition from the single-cell organism to the multicellular organism, many genes evolved to regulate these cellular functions. One of these genes is the gene coding for a membrane-associated protein channel (the gap junction).[12] Gap-junctional intercellular communication (GJIC) involves two hemichannels or connexons,[13] and each connexon is composed of six basic protein subunits named connexin (Cx), which allow the cell–cell transfer of small molecules. Approximately 20 connexins are known, and they are expressed in a cell- and development-specific manner.[14,15] GJIC also plays an important role in the maintenance of cell homeostasis and in the control of cell growth.[16] Thus, disruption of GJIC has been shown to contribute to the multi-step, multi-mechanism process of carcinogenesis.[17–19] Several tumor-promoting agents have been shown to restrict GJIC by phosphorylation of connexin proteins, such as connexin 43, which is essential in forming the gap junction channel.[20,21] Our previous study revealed that PLLA increased the secretion of transforming growth factor-β1 (TGF-β1), suppressed the mRNA expression of Cx 43, and inhibited GJIC in the early stage after implantation, thus promoting tumorigenesis in BALB/cJ mice.[22] We have hypothesized that the difference in tumorigenic potentials of PLLA is caused mainly by the different tumor-promoting activities of these biomaterials and that TGF-β1 might have an important role in PLLA-implanted BALB/cJ mice. Therefore, in our present experimental approach, we aimed to determine the novel effects of PLLA plates in two mouse strains, BALB/cJ and SJL/J, after long-term implantation. Among mouse strains, the former is a more tumorigenic strain when compared with the later.[23]

Correspondence to: T. Tsuchiya; e-mail: tsuchiya@nihs.go.jp
Contract grant sponsors: Ministry of Health, Labour and Welfare and Japan Health Sciences Foundation

© 2006 Wiley Periodicals, Inc.

Immune-deficient nude mice, which are highly susceptible to tumorigenicity, were also used in this experiment.

MATERIALS AND METHODS

Animals

Five-week-old female BALB/cJ and SJL/J, and five-week-old male BALB/cAnCrj-nu mice were purchased from Charles River (Japan) and maintained in the animal center according to the NIHS animal welfare guidelines. All mice were fed standard pellet diets and water *ad libitum* before and after PLLA implantation.

Implantation of PLLA

PLLA was obtained from Shimadzu Co. Ltd. as uniform sheets. The implants (size, 20 × 10 × 1 mm^3; Mw, 200,000) were sterilized using ethylene oxide gas prior to use. Sodium pentobarbital (4 mg/kg) was intraperitoneally administered to the mice. The dorsal skin was shaved and scrubbed with 70% alcohol. Using an aseptic technique, an incision of about 2 cm was made; a subcutaneous pocket was formed by blunt dissection away from the incision, and one piece of PLLA was placed in the pocket. The incision was closed with silk sutures. In both strains, controls were obtained by sham operation and subsequent subcutaneous pocket formation. Following surgery, the mice were housed in individual cages. After 10 months, mice from the implanted group were killed, implanted materials were excised, and subcutaneous tissues from the adjacent sites were collected for culture. At the same time, subcutaneous tissues were removed from the sites in the sham-operated controls that correlated with the implant sites. Similar experiments were also performed 1 month after PLLA implantation.[22]

Cell culture of subcutaneous tissues

The subcutaneous tissues were maintained in minimum essential medium (MEM) supplemented with 10% FBS in a 5% CO_2 atmosphere at 37°C.

Giemsa staining

When cells reached confluence in tissue culture dishes, they were fixed and stained with Giemsa solution. Cell morphology was determined under an inverted light microscope.

Western blot analysis

When cells had grown confluent in 60-mm tissue culture dishes, all cells were lysed directly in 100 μL 2% sodium dodecyl sulfate (SDS) gel loading buffer (50 m*M* Tris-HCl, pH 6.8, 100 m*M* 2-mercaptoethanol, 2% SDS, 0.1% bromophenol blue, and 10% glycerol). The protein concentration of the cleared lysate was measured using a micro-plate BCA protein assay (Pierce, Rockford, IL). Equivalent protein samples were analyzed by 7.5% SDS-polyacrylamide gel electrophoresis. The proteins were transferred to Hybond-ECL nitrocellulose membranes (Amersham Pharmacia Biotech UK, Buckinghamshire, UK), and Cx 43 protein was detected by anti-Cx 43 polyclonal antibodies (ZYMED Laboratories, San Francisco, CA). The membrane was soaked with Block Ace (Yukijirushi Nyugyo, Sapporo, Japan), reacted with the anti-Cx 43 polyclonal antibodies for 1 h, and after washes with phosphate-buffered saline (PBS) containing 0.1% Tween20, reacted with the secondary anti-rabbit IgG antibody conjugated with horseradish peroxidase for 1 h. After several washes with PBS-Tween20, the membrane was detected with the ECL detection system (Amersham Pharmacia Biotech UK).

Scrape-loading and dye transfer assay

The scrape-loading and dye transfer (SLDT) technique was performed by the method of El-Fouly et al.[24] Confluent monolayer cells in 35-mm culture dishes were used. After rinsing with Ca^{2+}, Mg^{2+} PBS(+), cell dishes were loaded with 0.1% Lucifer Yellow (Molecular Probes, Eugene, OR) in PBS(+) solution and were scraped immediately with a sharp blade. After incubation for 5 min at 37°C, cells were washed three times with PBS(+), and the extent of dye transfer was monitored using a fluorescence microscope equipped with a type UFX-DXII CCD camera and a super high-pressure mercury lamp power supply (Nikon, Tokyo, Japan).

Enzyme-linked immunosorbent assay

Cells were seeded onto 60-mm dishes. The conditioned medium was collected after centrifugation at 1000 rpm for 2 min. The TGF-β1 levels of the media were measured with commercially available enzyme linked immunosorbent assay (ELISA) kits (R&D Systems, Minneapolis, MN).

DNA microarray analysis

At least 10^7 cells were harvested and frozen in liquid nitrogen. Total RNA was extracted, purified, and assessed for yield and purity, and cDNA probes were synthesized with the Atlas™ Pure Total RNA Labeling System (Clontech) according to the manufacturer's instructions. Hybridization of the ^{33}P-labeled probes to the Atlas Array of Mouse Cancer 1.2 k Array (Clontec 7858–1), on which 1176 cDNAs

of cancer-related genes were spotted, was performed with Atlas™ cDNA Expression Arrays according to the manufacturer's instructions. The phosphor images of hybridized arrays were analyzed with AtlasImage™ (Clontech). Genes that were up- or downregulated more than fivefold relative to the negative controls are discussed.

Determination of tumorigenicity in nude mice

Cultured cells were harvested by trypsinization, and 2×10^6 washed cells suspended in 0.2 mL of PBS were inoculated at a single subcutaneous site into 6–8-week-old nude mice. All mice were examined regularly for the development of tumor.

Soft agar assay

Approximately 100,000 cells per well from each clone were seeded in 2 mL of 0.3% soft agar in culture medium on a solidified basal layer in 6-well tissue culture plates. The plates were cultured for 4 weeks and then stained with *p*-iodotetrazolium violet for 48 h before counting.

Statistical analysis

Student *t* tests were used to assess whether differences observed between the implanted and control samples were statically significant. For comparison of groups of means, one-way analysis of variance was carried out. When significant differences were found, Tukey's pairwise comparisons were used to investigate the nature of the difference. The confidence level was set at 95% for all tests. Statistical significance was accepted at $p < 0.05$. Values were presented as the mean ± SD.

RESULTS

Giemsa staining

Cells with different morphologies formed a slightly crisscrossed pattern in the BALB/cJ control group, whereas cells in the implanted groups of BALB/cJ showed a markedly crisscrossed pattern. The cells were extensively piled up, which decreased contact inhibition, under inverted light microscopy observation and Giemsa staining [Fig. 1(A,B)]. In contrast, the cells of the SJL/J group formed a parallel, flat, confluent monolayer that maintained contact inhibition [Fig. 1(C,D)].

Western blot analysis

We examined the protein expression of the connexin 43 gene and found that the total protein level was significantly decreased in PLLA-implanted BALB/cJ mice when compared with that in BALB/cJ controls (Fig. 2). However, protein expression was decreased in both control and PLLA-implanted groups in SJL/J mice (Fig. 2).

SLDT assay

The SLDT assay was used to assess functional GJIC. GJIC was significantly inhibited in PLLA-implanted BALB/cJ mice when compared with that in BALB/cJ controls (Fig. 3). A significant difference was also observed between the two strains of mice in that the GJIC was lower in SJL/J than in BALB/cJ group (Fig. 3).

ELISA

The secretion of TGF-β1 was significantly increased in PLLA-implanted BALB/cJ subcutaneous tissues in comparison with that from BALB/cJ control mice. On the contrary, secretion of TGF-β1 tended to decrease in the SJL/J implanted mice when compared with that in SJL/J control mice (Fig. 4).

DNA microarray analysis of the four kinds of cells

Expression of the major ECM [fibronectin 1, procollagen VIIIα 1, and osteopontin precursor (OPN)] proteins [Fig. 5(A–C)], insulin-like growth factor-binding protein (IGFBP) 3 [Fig. 5(D)], and cysteine-rich intestinal protein 2 (CRIP 2) [Fig. 5(E)] were increased in the PLLA-implanted BALB/cJ mouse cells when compared with that in BALB/cJ control mouse cells. No such difference was observed between SJL/J implanted and control mouse cells.

Tumorigenicity in nude mice

No tumor was formed in PBS(−) injected nude mice [Fig. 6(A)]. Rapid growth of large tumors was observed in nude mice within 2 weeks of injection of cultured cells from PLLA-implanted BALB/cJ mice [Fig. 6(B,C,E,F)]. Nude mice injected with HeLa cells, which served as positive controls, showed slower growth of tumor 4 weeks after cell injection [Fig. 6(D,G)].

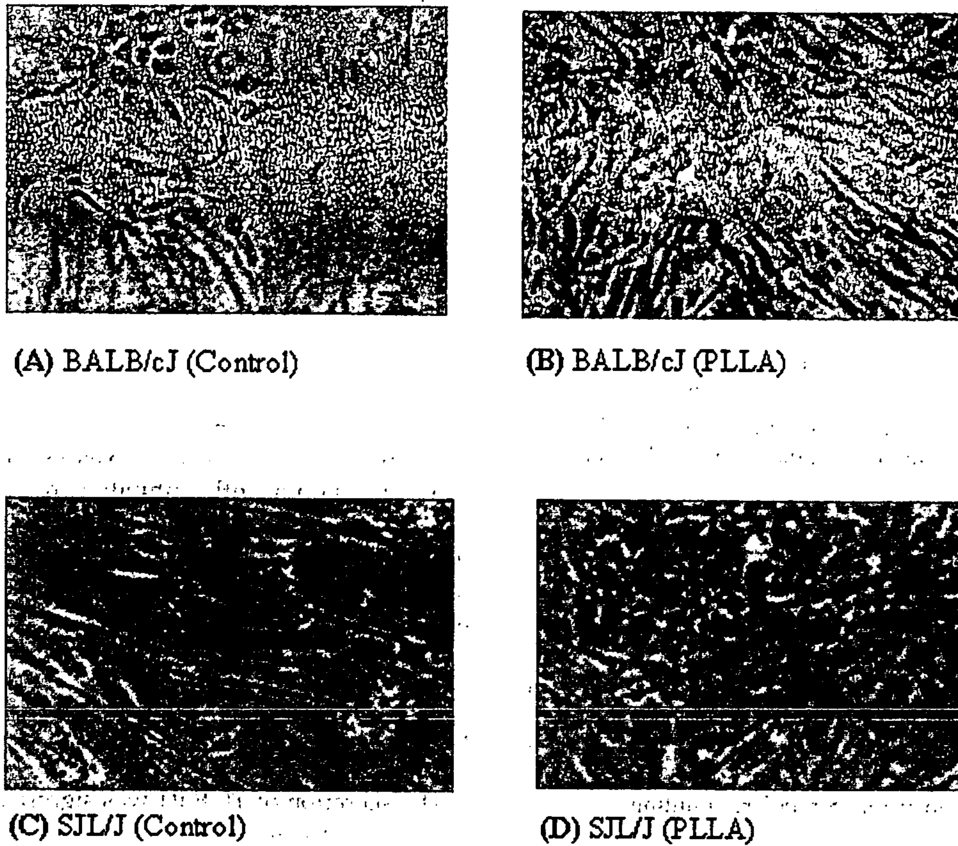

Figure 1. Mouse cell morphology. Three each of both implanted mice and sham-operated controls were killed after 10 months. Results shown are representative of two independent experiments. Inverted light microscopic appearance (magnification ×100) of (A) BALB/cJ (control), (B) BALB/cJ (PLLA), (C) SJL/J (control), and (D) SJL/J (PLLA). [Color figure can be viewed in the online issue, which is available at www.interscience.wiley.com.]

Soft agar assay

These tumor cells did not form a colony in soft agar (data not shown), although HeLa cells did form colonies in soft agar.

Histopathology

Tumor cells from nude mice injected with PLLA-implanted BALB/cJ mouse cells showed monophasic

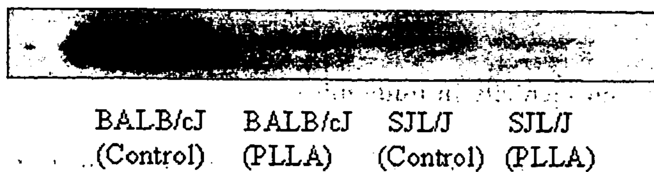

Figure 2. Expression of Cx 43 protein by Western blot analysis. Three each of both implanted mice and sham-operated controls were killed after 10 months. Results shown are representative of two independent experiments. Total protein expression was significantly decreased in PLLA-implanted BALB/cJ mice when compared with that in the control. However, protein expression was decreased in both control and PLLA-implanted groups in SJL/J mice.

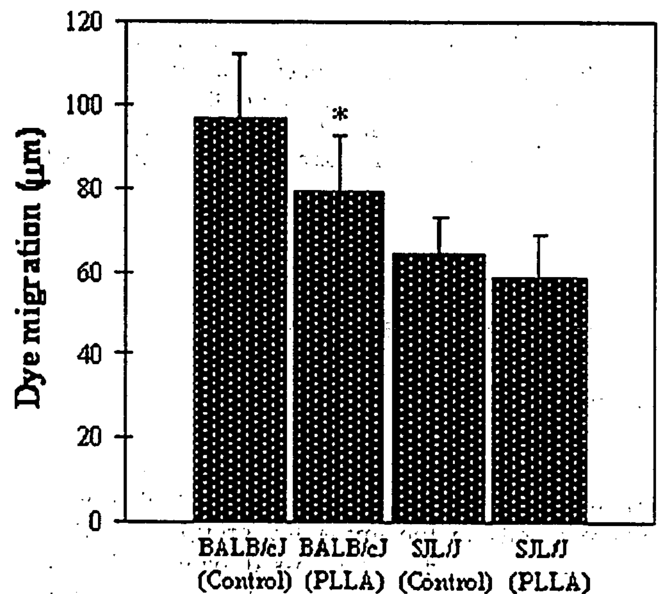

Figure 3. Statistical analysis of SLDT assay. Three each of both implanted mice and sham-operated controls were killed after 10 months. Results shown are representative of two independent experiments. GJIC was found to be significantly inhibited in PLLA-implanted BALB/cJ mice cells when compared with that in BALB/cJ controls. $^{*}p < 0.05$.

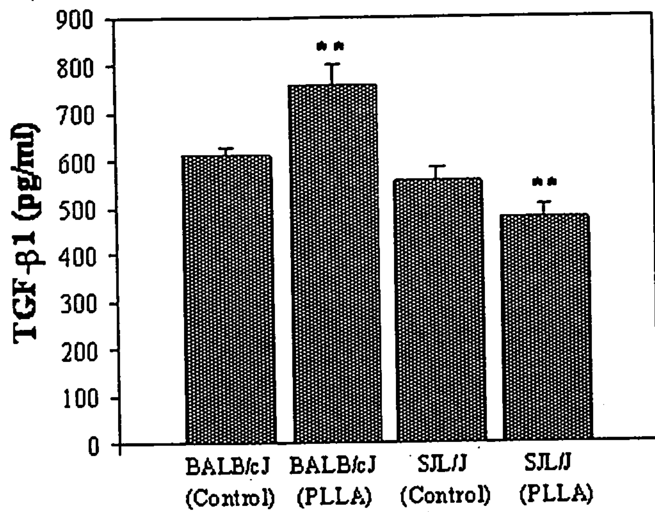

Figure 4. Statistical analysis of TGF-β1 cytokine assay by ELISA. Three each of both implanted mice and sham-operated controls were killed after 10 months. Results shown are representative of two independent experiments. Secretion of TGF-β1 level was significantly increased in PLLA-implanted BALB/cJ mice when compared with that in BALB/cJ controls. On the contrary, in the SJL/J mice, secretion of TGF-β1 tended to decrease in PLLA-implanted mice when compared with that in control mice. $^{**}p < 0.01$.

fibrous synovial sarcoma on H&E and keratin AE1/AE3 staining. Tumor cells with a staghorn pattern [Fig. 7(A)] and a herringbone pattern were identified [Fig. 7(B,C)].

DISCUSSION

Polylactides are bioabsorbable polyesters with wide range of clinical applications. Because it degrades slowly, PLLA has been used as a biomaterial for surgical devices such as bone plates, pins, and screws. It has been reported in different studies that polyetherurethane, nonabsorbable polyethylene, and PLLA produced tumors in rats.[9,10,25–27] Parallel to these studies, here cells with different morphologies formed a crisscross pattern, which thus decreased the contact inhibition in the PLLA-implanted BALB/cJ group [Fig. 1(B)]. We examined the protein expression of Cx 43 to evaluate the actual cause and found that the total level of protein expression was significantly decreased in the PLLA-implanted groups when compared with that in the controls (Fig. 2). In contrast, Cx 43 protein expression was decreased in both control

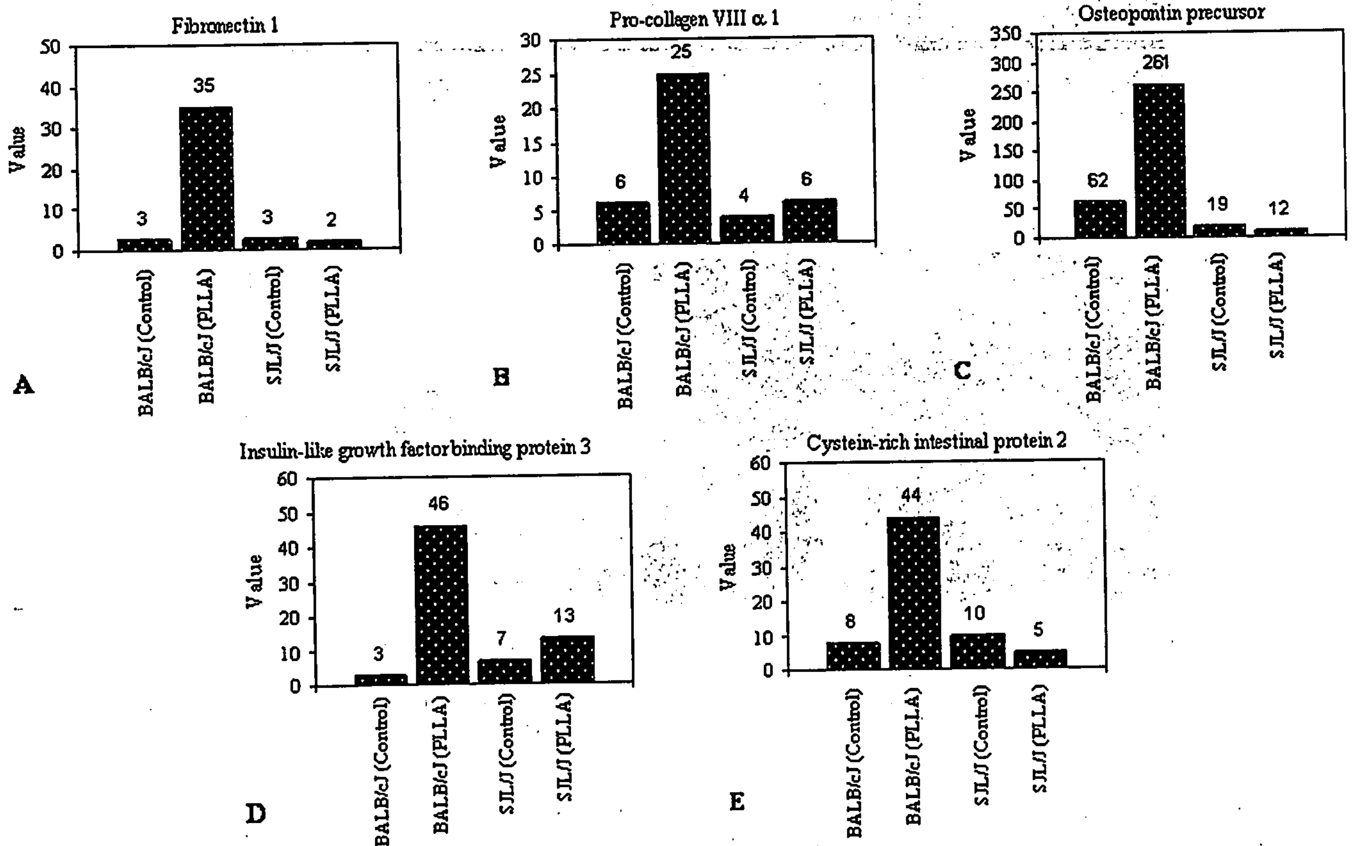

Figure 5. DNA microarray analysis of these four kinds of cells. The expression of (A) fibronectin 1, (B) pro-collagen VIIIα 1, (C) osteopontin precursor (OPN), (D) insulin-like growth factor binding protein (IGFBP) 3, and (E) cysteine-rich intestinal protein 2 (CRIP 2) increased in the cells of PLLA-implanted BALB/cJ mice. Results shown are representative of four independent experiments.

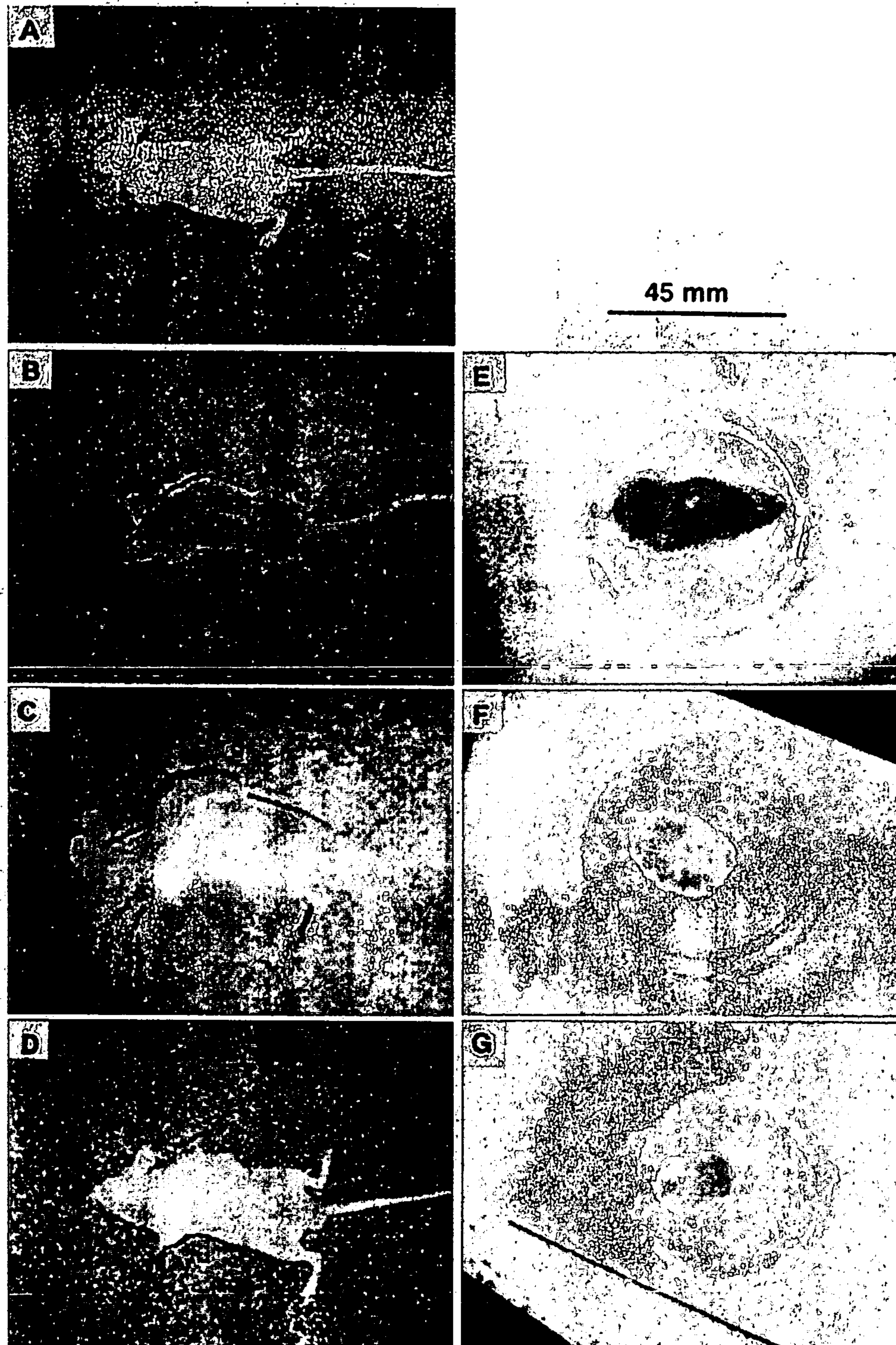

Figure 6. Determination of tumorigenicity in nude mice. (A) No tumor was formed in PBS(−) injected nude mice. (B, C, E, and F) A large tumor growth was observed within two weeks in nude mice injected with cells from PLLA-implanted BALB/cJ mice. (D and G) Tumor growth was observed in nude mice 4 weeks after they were injected with HeLa cells. [Color figure can be viewed in the online issue, which is available at www.interscience.wiley.com.]

and PLLA-implanted groups in SJL/J mice (Fig. 2). We also examined the functional effects on GJIC. In the present study and correlating with our previous report,[22] GJIC was significantly inhibited in PLLA-implanted BALB/cJ mice when compared with that in controls (Fig. 3). Gap junctions are regulated by the post-translational phosphorylation of the carboxy-terminal tail region on the Cx molecule, and hyperphosphorylation of Cx molecules is closely related to the inhibition of GJIC.[28,29] Asamoto et al. reported that tumorigenicity enhanced when the expression of Cx 43 protein was suppressed by the anti-sense RNA of

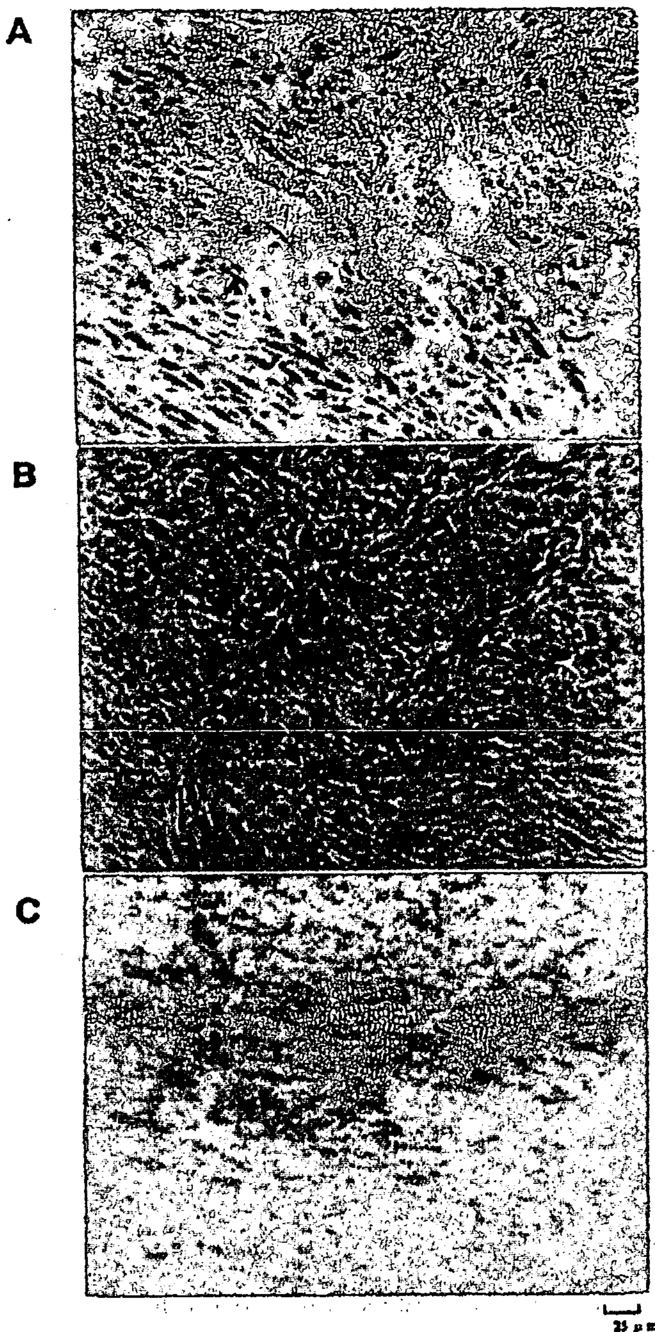

Figure 7. Histopathology. Tumor cells from nude mice injected with cells from PLLA-implanted BALB/cJ mice showed monophasic fibrous synovial sarcoma with H&E and keratin AE1/AE3 staining. (A) Staghorn pattern (H&E), (B) herringbone pattern (H&E), and (C) herringbone pattern (keratin AE1/AE3 staining). [Color figure can be viewed in the online issue, which is available at www.interscience.wiley.com.]

Cx 43.[30] Thus, in our experiment, the impaired GJIC was possibly caused by the suppression of protein expression of Cx 43. Therefore, it is suggested that gap junctions are likely to play a major role in the PLLA-induced tumorigenesis in BALB/cJ mice. But in SJL/J mice, this is not the key factor for tumorigenesis. Another protein may be responsible because Cx 43 protein expression was decreased in both control and PLLA-implanted group of SJL/J mice.

TGF-β1 can impair GJIC function by decreasing the phosphorylated form of Cx 43[31] and can also increase the expression of ECM.[32,33] We estimated the production of TGF-β1 in four kinds of cells. The secretion of TGF-β1 significantly increased in PLLA-implanted BALB/cJ mice cells in comparison with that from BALB/cJ control mice, but TGF-β1 secretion decreased in the SJL/J-implanted group when compared with that in the SJL/J control mice (Fig. 4). Furthermore, by using DNA microarray analysis of these four kinds of cells, expression of the major ECM proteins (fibronectin 1, pro-collagen VIIIα 1, and OPN) and IGFBP 3 was found to be increased in the PLLA-implanted BALB/cJ mice cells (Fig. 5). Several reports have suggested that these proteins could directly cause tumorigenesis.[34–36] Overexpression of CRIP 2, a member of the LIM (characterized by a repeat of a double zinc finger cysteine-rich sequence, CCHC and CCCC) protein family, caused an increase in Th2 cytokine IL-6,[37] and synovial sarcoma cells are reported to produce IL-6 by themselves.[38] Figure 5 shows that IGFBP 3 was highly expressed in the PLLA-implanted BALB/cJ mice cells. In addition, overexpression of IGFBP 3 was associated with poorer prognosis in breast cancer.[36] Therefore, we speculated that overexpression of IGFBP 3 and major ECM proteins directly or indirectly causes tumorigenesis in the PLLA-implanted BALB/cJ mice.

Ten months after implantation of the PLLA plate into BALB/cJ mice, formation of a tissue growth was observed at the implanted site. To determine whether this tissue growth was a tumor or a result of foreign body (PLLA) inflammation, we performed a tumorigenicity assay in nude mice. Rapid growth of a large tumor was observed in nude mice injected with cells obtained from PLLA-implanted BALB/cJ mice (Fig. 6). The histopathologic examination of this tumor disclosed monophasic fibrous synovial sarcoma (Fig. 7). Nude mice injected with HeLa cells as a positive control showed slower tumor growth. However, these PLLA-derived tumor cells did not form a colony in a soft agar assay (data not shown).

We speculated that a protein or regulatory factor other than Cx 43 may play key role in tumorigenesis in PLLA-implanted BALB/cJ mice. In this light, we conclude that overexpression of the regulatory factors such as TGF-β1 and IGFBP 3 caused tumorigenesis in PLLA-implanted BALB/cJ mice. In addition, increased secretion of TGF-β1 suppressed the expression of Cx 43 and inhibited GJIC. Moreover, PLLA increased the expression of ECM, CRIP 2, and OPN. Finally, all these factors in combination promoted tumorigenesis (Fig. 8).

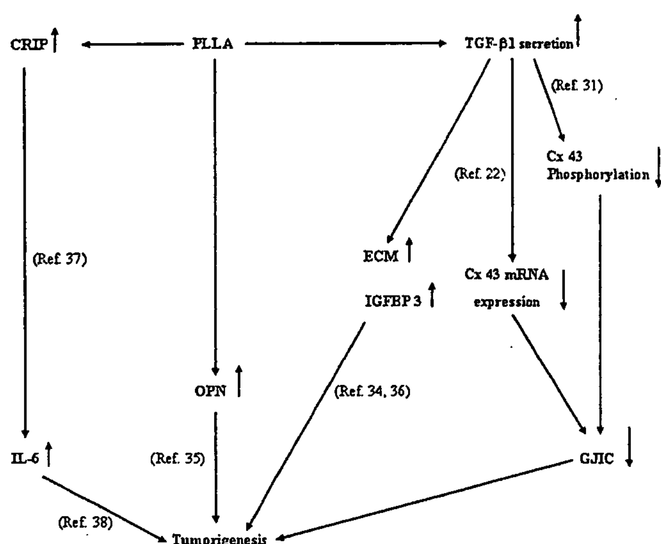

Figure 8. Schematic representation of the pathway of tumorigenesis induced by PLLA in BALB/cJ mice.

References

1. Hayashi T. Interactions between polymers and biosystems: Structure–property relationships in biomaterial polymers. In: Thuruta T, Hayashi T, Kataoka K, Ishihara K, Kimura Y, editors. Biomaterial Applications of Polymeric Materials. Boca Raton, FL: CRC; 1993. pp 17–51.
2. Chesmel KD, Black J. Cellular responses to chemical and morphologic aspects of biomaterial surfaces. I. A novel in vitro model system. J Biomed Mater Res 1995;29:1089–1099.
3. Tang L, Eaton JW. Inflammatory responses to biomaterials. Am J Clin Pathol 1995;103:466–471.
4. Imai Y. Interaction between polymers and biosystem: Biological response to biomedical polymers. In: Thuruta T, Hayashi T, Kataoka K, Ishihara K, Kimura Y, editors. Biomaterial Applications of Polymeric Materials. Boca Raton, FL: CRC; 1993. pp 53–87.
5. Rosengren A, Danielson N, Bjursten LM. Inflammatory reaction dependence on implant localization in rat soft tissue models. Biomaterials 1997;18:979–987.
6. Butler K, Benghuzzi H, Tucci M, Cason Z. A comparison of fibrous tissue formation surrounding intraperitoneal and subcutaneous implantation of ALCAP, HA, and TCP ceramic devices. Biomed Sci Instrum 1997;34:18–23.
7. Kulkarni RK, Pani KC, Neuman C, Leonard F. Polylactic acid for surgical implants. Arch Surg 1966;93:839–843.
8. Craig PH, Williams JA, Davis KW, Magoun AD, Levy AJ, Bogdansky S, Jones JP Jr. A biological comparison of polyglactin 910 and polyglycolic acid synthetic absorbable sutures. Surg Gynecol Obstet 1995;141:1–10.
9. Nakamura T, Shimizu Y, Okumura N, Matsui T, Hyon SH, Shimamoto T. Tumorigenicity of poly-L-lactide (PLLA) plates compared with medical-grade polyethylene. J Biomed Mater Res 1994;28:17–25.
10. Nakamura A, Kawasaki Y, Takada K, Aida Y, Kurokama Y, Kojima S, Shintani H, Matsui M, Nohmi T, Matsuoka A, Sofuni T, Kurihara M, Miyata N, Uchima T, Fujimaki M. Difference in tumor incidence and other tissue responses to polyetherurethanes and polydimethylsiloxane in long-term subcutaneous implantation into rats. J Biomed Mater Res 1992;26:631–650.
11. Trosko JE, Madhukar BV, Chang CC. Endogenous and exogenous modulation of gap junctional intercellular communication: Toxicological and pharmacological implications. Life Sci 1993;53:1–19.
12. Trosko JE, Ruch RJ. Cell–cell communication in carcinogenesis. Front Biosci 1998;3:D208–D236.
13. Falk MM. Biosynthesis and structural composition of gap junction intercellular membrane channels. Eur J Cell Biol 2000;79: 564–574.
14. Evans WH, Martin PE. Gap junctions: Structure and function. Mol Membr Biol 2002;19:121–136. Review.
15. Bruzzone R, White TW, Paul DL. Connections with connexins: The molecular basis of direct intercellular signaling. Eur J Biochem 1996;238:1–27.
16. Loewenstein WR. Junctional intercellular communication and the control of growth. Biochim Biophys Acta 1979;560:1–65.
17. Guthrie SC, Gilula NB. Gap junctional communication and development. Trends Neurosci 1989;12:12–16.
18. Klaunig JE, Ruch RJ. Role of inhibition of intercellular communication in carcinogenesis. Lab Invest 1990;62:135–146.
19. Mesnil M, Yamasaki H. Cell–cell communication and growth control of normal and cancer cells: Evidence and hypothesis. Mol Carcinog 1993;7:14–17.
20. Musil LS, Goodenough DA. Biochemical analysis of connexin43 intracellular transport, phosphorylation, and assembly into gap junctional plaques. J Cell Biol 1991;115:1357–1374.
21. Musil LS, Goodenough DA. Multisubunit assembly of an integral plasma membrane channel protein, gap junction connexin43, occurs after exit from the ER. Cell 1993;74:1065–1077.
22. Ahmed S, Tsuchiya T. A novel mechanism of tumorigenesis: Increased TGF-β1 suppresses the expression of connexin43 in BALB/cJ mice after implantation of PLLA. J Biomed Mater Res A 2004;70:335–340.
23. Brand I, Buoen LC, Brand KG. Foreign-body tumors of mice: Strain and sex differences in latency and incidence. J Natl Cancer Inst 1977;58:1443–1447.
24. El-Fouly MH, Trosko JE, Chang CC. Scrape-loading and dye transfer. A rapid and simple technique to study gap junctional intercellular communication. Exp Cell Res 1987;168:422–430.
25. Tsuchiya T, Hata H, Nakamura A. Studies on the tumor-promoting activity of biomaterials: Inhibition of metabolic cooperation by polyetherurethane and silicone. J Biomed Mater Res 1995;29:113–119.
26. Tsuchiya T. A useful marker for evaluating tissue-engineered products: Gap-junctional communication for assessment of the tumor-promoting action and disruption of cell differentiation in tissue-engineered products. J Biomater Sci Polym Ed 2000; 11:947–959.
27. Nakaoka R, Tsuchiya T, Kato K, Ikada Y, Nakamura A. Studies on tumor-promoting activity of polyethylene: Inhibitory activity of metabolic cooperation on polyethylene surfaces is markedly decreased by surface modification with collagen but not with RGDS peptide. J Biomed Mater Res 1997;35:391–397.
28. Musil LS, Cunningham BA, Edelman GM, Goodenough DA. Differential phosphorylation of the gap junction protein connexin43 in junctional communication-competent and -deficient cell lines. J Cell Biol 1990;111:2077–2088.
29. Lampe PD, Lau AF. Regulation of gap junctions by phosphorylation of connexins. Arch Biochem Biophys 2000;384: 205–215.
30. Asamoto M, Toriyama-Baba T, Krutovskikh V, Cohen SM, Tsuda H. Enhanced tumorigenicity of rat bladder squamous cell carcinoma cells after abrogation of gap junctional intercellular communication. Jpn J Cancer Res 1998;89:481–486.
31. Wyatt LE, Chung CY, Carlsen B, Iida-Klein A, Rudkin GH, Ishida K, Yamaguchi DT, Miller TA. Bone morphogenetic protein-2 (BMP-2) and transforming growth factor-β1 (TGF-β1) alter connexin 43 phosphorylation in MC3T3–E1 Cells. BMC Cell Biol 2001;2:14.

32. Singh LP, Green K, Alexander M, Bassly S, Crook ED. Hexosamines and TGF-β1 use similar signaling pathways to mediate matrix protein synthesis in mesangial cells. Am J Physiol Renal Physiol 2004;286:F409–F416.
33. Kenyon NJ, Ward RW, McGrew G, Last JA. TGF-β1 causes airway fibrosis and increased collagen I and III mRNA in mice. Thorax 2003;58:772–777.
34. Kuchenbauer F, Hopfner U, Stalla J, Arzt E, Stalla GK, Paez-Pereda M. Extracellular matrix components regulate ACTH production and proliferation in corticotroph tumor cells. Mol Cell Endocrinol 2001;175:141–148.
35. Liu SJ, Hu GF, Liu YJ, Liu SG, Gao H, Zhang CS, Wei YY, Xue Y, Lao WD. Effect of human osteopontin on proliferation, transmigration and expression of MMP-2 and MMP-9 in osteosarcoma cells. Chin Med J (Engl) 2004;117:235–240.
36. Rocha RL, Hilsenbeck SG, Jackson JG, VanDenBerg CL, Weng C, Lee AV, Yee D. Insulin-like growth factor binding protein-3 and insulin receptor substrate-1 in breast cancer: Correlation with clinical parameters and disease-free survival. Clin Cancer Res 1997;3:103–109.
37. Cousins RJ, Lanningham-Foster L. Regulation of cysteine-rich intestinal protein, a zinc finger protein, by mediators of the immune response. J Infect Dis 2000;182:S81–S84.
38. Duan Z, Lamendola DE, Penson RT, Kronish KM, Seiden MV. Overexpression of IL-6 but not IL-8 increases paclitaxel resistance of U-2OS human osteosarcoma cells. Cytokine 2002;17:234–242.

Key Engineering Materials Vols. 309-311 (May 2006) pp. 97-100
online at http://www.scientific.net
© 2006 Trans Tech Publications, Switzerland

Novel Calcium Phosphate Ceramics : The Remarkable Promoting Action on the Differentiation of the Normal Human Osteoblasts

Masato Tamai[1a], Ryusuke Nakaoka[1b], Kazuo Isama [1c] and Toshie Tsuchiya[1d]
[1]Division of Medical Devices, National Institute of Health Sciences,
1-18-1 Kamiyoga, Setagaya-ku, Tokyo 158-8501 Japan
[a]m-tamai@nihs.go.jp, [b]nakaoka@nihs.go.jp, [c]isama@nihs.go.jp, [d]tsuchiya@nihs.go.jp

Keywords: Hydroxyapatite, Niobium ion, Osteoblast, Alkaline phosphatase activity

Abstract.
To promote the activity of normal human osteoblasts (NHOst), the novel HAp ceramics containing Nb ions (NbHAp) were synthesized by wet chemical process, which reacting aqueous solution containing a mixture of $Ca(NO_3)_2$, $(NH_4)_2HPO_4$, and the Nb aqueous solution. X-ray diffraction patterns indicated that NbHAp had a monolithic apatitic structure, although crystallite decreased as Nb content increased. From inductively coupled plasma analysis, maximum amount of Nb ions in the sample was almost 8.2atom% of P ions. The NbHAps were presented as aggregates and composed of fine crystal of <1μm in diameter. Nb ions in NbHAp were uniformly distributed in the aggregates. Furthermore, high-resolution XPS spectra of Nb $3d_{5/2}$ indicated that Nb ions in the HAp were presented as Nb^{5+}. These results suggested that Nb ions were at PO_4 site in crystal structure of HAp. When NHOst were cultured with the NbHAp, their ALP activity were twice as much as that of NHOst cultured with HAp without Nb ions.

Introduction

Tissue engineering takes advantages of the combined use of cultured living cells and scaffolds to deliver vital cells to the damaged site of the patient. Some tissue engineering approaches have been devised to repair large bone defect. In developing of the scaffold for bone tissue, the interaction between osteoblasts cells and scaffolds are much important. To achieve the restoration the bone tissue at early stage, the scaffold is required to have the ability of promoting proliferation and mineralization.

It is well known that hydroxyapatite ($Ca_{10}(PO_4)_6(OH)_2$, HAp) ceramics can be biologically bonded to natural bones and have been studied to utilize as the scaffolds. In addition, the structure is very tolerant of ionic substitutions and Ca^{2+} ions, PO_4^{3-} ions and OH^- ions can be replaced by various cationic or anionic ions, partly or completely[1]. For example, K^+, Mg^{2+} and Sb^{3+}, can substituted for Ca ions and CO_3^{2-} and VO_4^{3-} can substituted for PO_4^{3-} ions, completely or partially. Thus various kinds of ion substitutions can be made to synthesize novel modified-HAps.

Recently, our co-workers reported that niobium (Nb) ions have the significant effect which promotes the proliferation and differentiation of normal human osteoblastic cells (NHOst)[2]. In the present study, therefore, we attempted to synthesize the novel HAp ceramics containing Nb ions (NbHAp) to promote the activity of NHOst and investigated the interaction between NbHAp and NHOst.

Materials and Methods

Synthesis of Nb containing HAp

The NbHAp was synthesized by wet chemical process, which reacting aqueous solution containing a mixture of $Ca(NO_3)_2$, $(NH_4)_2HPO_4$, and the Nb aqueous solution. The reagent grade $Ca(NO_3)_2$, $(NH_4)_2HPO_4$ and $NbCl_5$ (Wako Pure Chemical Industries, Ltd) were used without purification. The metal ion chemical reagent was completely dissolved in an exact amount of distilled water. The Nb aqueous solution was prepared by the mixing of distilled water and $NbCl_5$ solution, which dissolved in 5vol%-hydroxyaceton and 5vol%-2-aminoethanol[3].

0.2M-$(NH_4)_2HPO_4$ and 0.01M $NbCl_5$ solutions were mixed and stirred with a magnetic bar. The Nb/(Nb+P) molar ratio of the mixing solution was set to 0.0000, 0.0167 and 0.1667. The pH of the mixing solution was adjusted to 10 using 1N-NaOH. 0.2M-$Ca(NO_3)_2$ was slowly dropped in the mixing solution (20ml/min) The ionic content of those starting solutions are shown in table 1. The pH was monitored and the reaction was terminated at pH 10.0. After the reaction, the suspension was stirred for 24h at room temperature. The precipitates were centrifuged at 3000rpm for 5min and washed with distilled water. The obtained apatites were annealed at 800°C for 2h (heating rate: 5°C/min). In this study, those precipitates obtained by reaction of $Ca(NO_3)_2$ solution and the mixing solution with different Nb/(Nb+P) molar ratio of 0.000, 0.0167 and 0.1667 are named HAp , NbHAp-I and NbHAp-II, respectively.

Characterization of NbHAp

The NbHAps were characterized by X-ray diffraction analysis (XRD, Rigaku, Rint2000). Ca, P and Nb ions concentrations in apatites are measured by inductively coupled plasma (ICP, Hewlett-Packard, HP4500).. Microstructural evaluation was performed by scanning electron microscopy (SEM) and energy dispersive X-ray spectroscopy (EDS) (JEOL, LV5800). The chemical state of Nb ions in HAp was investigated by X-ray photon spectroscopy (XPS, Shimadzu, ESCA-3200).

Osteogenesis evaluation of NHOst cultured with NbHAp

NHOst were purchased from BioWhittaker Inc.(Walkersville,MD). The NHOst were maintained in alpha minimum essential medium (αMEM, Gibco, Grand Island, NY) containing 10%-FCS in incubators at 37°C in a humidified atmosphere with 5% CO_2. All assays were performed using αMEM containing 10%-FCS supplemented with 10mM beta-glycerophosphate. NHOst cells (4×10^4 cells/well/ml) were co-cultured with 5mg of the apatites for 7days to evaluated the effects of the apatites on NHOst.

Proliferation of NHOst cells cultured with the apatites was estimated by Tetracolor One assay (Seikagaku Co., Ltd. Tokyo, Japan), which incorporates an oxidation reduction indicator based on detection of metabolic activity. After 7-days incubation, 2%-TetraColor One/αMEM solution was added to each well, followed by 2h incubation. The absorbance of the supernatant at 450nm was estimated using μQuant spectrophotometer (Bio-tek Instrument, Inc., Winooski, VT). After estimating the proliferation, the cells were washed by phosphate–buffered saline (PBS(-)), followed by addition of 1ml of 0.1M glycine buffer (pH=10.5) containing 10mM $MgCl_2$, 0.1mM $ZnCl_2$ and 4mM p-nitrophenylphosphate sodium salt. After incubating at room temperature for 5min, the absorbance at 405 nm was detected using the μQuant spectrophotometer to evaluated alkaline phosphatase (ALP) activity of the test cells.

Results and Discussion

XRD patterns of NbHAps prepared by wet chemical process are shown in Fig.1(a). Irrespective of Nb/(Nb+P) molar ratio in starting solution, the precipitates were identified as monolithic HAp.

Table1. The ionic content of starting solution and the composition of the obtained precipitates.

Samples	Ionic content of Starting Solution*,			Theoretical Ca/(Nb+P)**	Nb/(Nb+P)**		Color of Precipitates
	Ca	PO_4	Nb		Theoretical	Measured***	
HAp	60.0	36.0	0.0	1.67	0.0000	-	White
NbHAp-I	60.0	35.4	0.6	1.67	0.0167	0.015	Pale yellow
NbHAp-II	60.0	30.0	6.0	1.67	0.1667	0.082	Buff yellow

*mmol, **Molar ratio, ***The precipitates were dissolved with HCl and the ionic concentration of HCl solutions were measured by ICP.

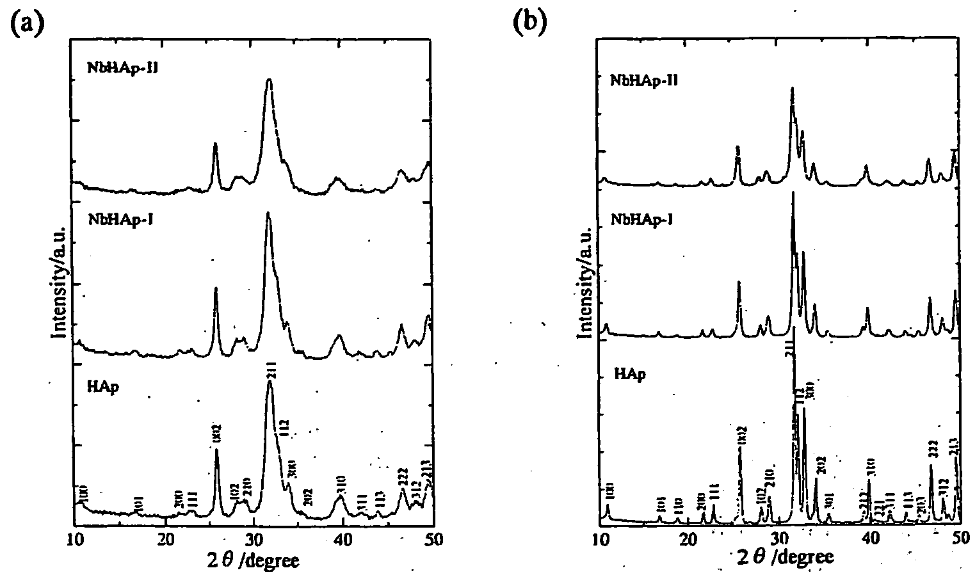

Fig.1. XRD patterns of HAp and NbHAp-I and NbHAp-II before (a) and after (b) annealing(800°C, 2h).

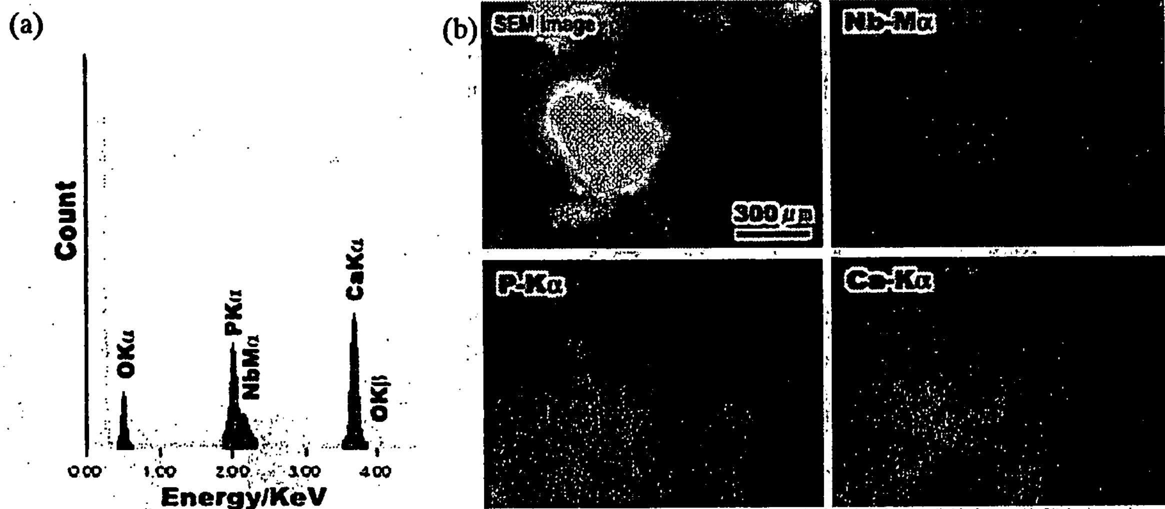

Fig.2. SEM-EDX analysis of NbHAp-II. ((a) An EDX spectrum and (b) SEM image and element mapping images of Nb, Ca and P).

As shown in Table1, the Nb/(Nb+P) molar ratio of NbHAp-I and NbHAp-II were 0.015 and 0.082, respectively. SEM observation revealed that the precipitates were present as aggregates composed of primary particles of less than 1μm in diameter.

XRD patterns of NbHAps annealed at 800°C are shown in Fig.1(b). The crystalline of the precipitates become high by the annealing and XRD patterns of all annealed NbHAps could be identified as monolithic apatitic structure. It is noted that the crystallite of the NbHAp decreased as Nb content increased. Figure 2(a) shows an EDX spectra of the whole region of SEM image in Fig.2(b). The EDX spectrum from Nb M_{α} was separated from P K_{α} line and could be observed at 2.17KeV, although the intensity of the spectra was weak. The mapping image of Nb, Ca and P ions are shown in Fig.2(b). As shown in Fig.2(b), Nb ions were present at the same site of Ca and P ions. Based on these observations, Nb ions are suggested to be uniformly distributed in the

aggregates. High-resolution XPS spectrum of Nb $3d_{5/2}$ of NbHAp-II annealed at 800°C is shown in Fig.3. The peak of XPS spectra due to $3d_{5/2}$ of Nb ions from annealed NbHAp-II is at 208.3eV. Since XPS peak of $3d_{5/2}$ due to Nb^{2+} from NbO and Nb^{5+} from Nb_2O_5 appears at 203.5eV and 207.2eV, respectively, the Nb ions in NbHAp can be identified as Nb^{5+}.

These results suggest that the NbHAp has apatitic structure containing Nb ions and the Nb ions are homogenously distributed in the grain. Generally, Nb^{5+} ions in the solution is not present as Nb^{5+} but as niobiumate acid, $H_xNb_6O_{19}{}^{(8-x)-}$ ions (X=0,1,2)[4]. The PO_4 in HAp can be replaced by anionic atomic group, e.g. $CO_3{}^{2-}$, $VO_4{}^{3-}$ and $AsO_4{}^{3-}$. Therefore, it is probable that Nb ions are substituted in PO_4 site in HAp. However, measured Nb/(Nb+P) molar ratio in NbHAp-II was 0.082, despite their theoretical Nb/(Nb+P) ratio of 0.1667, suggesting that the value of the measured ratio might be the maximum amount of Nb ions in PO_4, practically.

Since Nb ions are expected to have an effect to promote the proliferation and ALP activity of osteoblastic cells, the NbHAps have a potential to promote the ALP activity of osteoblastic cells.

Figure 4 shows ALP activity of NHOst cultured with annealed NbHAps. As shown in Fig.4, NHOst cultured with the NbHAp expressed the ALP activities twice as much as that of NHOst cultured with HAp without Nb ions. It is well known that ALP is often expressed when fracture of bone is repaired *in vivo*. Furthermore, from the recent study, it has revealed that the ALP contributed to mineralization in bone formation[5]. Therefore, this enhancement in ALP activity of NHOst by NbHAp suggests that the NbHAp can promote the mineralization of bone formation.

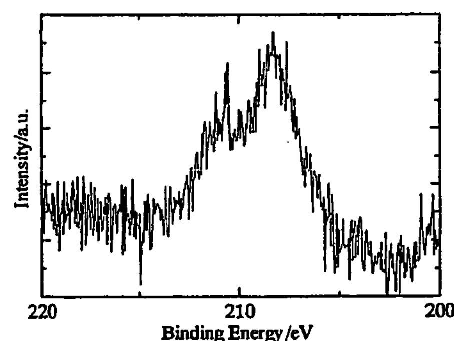

Fig.3. High-resolution XPS spectrum of Nb $3d_{5/2}$ of NbHAp-II annealed at 800°C.

Conclusion

We have succeeded to synthesize novel HAp containing Nb ions. The NbHAp would be a solid solution, which Nb ions were in PO_4 site in HAp and could enhance the ALP activity in NHOst.

Acknowledgment

This study was supported in part by a Grant-in-Aid for Scientific Research on Advanced Medical Technology from Ministry of Labour, Health and Welfare, Japan and a Grant-in-Aid from Japan Human Sciences Foundations.

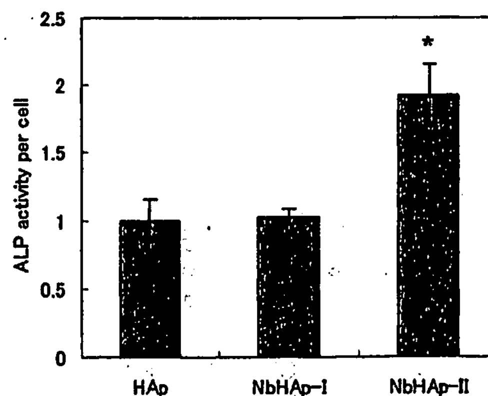

Fig.4. ALP activity of NHOst cultured with annealed NbHAp
*$p<0.05$ against HAp (without Nb ions)

References

[1] J.C.Elliott: *Structure and chemistry of the apatite and other calcium orthophosphates* (Elsevier, Tokyo, 1994)

[2] K.Isama, and T.Tsuchiya: Bull.Natl.Inst.Health.Sci., Vol.121 (2003) p.111

[3] T.Ohya, T.Ban, YOhya and Y.Takahashi: Ceram.Trans., Vol.112 (2001) p.47

[4] F.A.Cotton and G.Wilkinson: *Advanced Inorganic Chemistry* (Baifukan, Tokyo, 1994)

[5] H.Sowa, H.Kaji, T.Yamaguchi, T.Sugimoto and K.Ichihara: J.Bone.Miner.Res. Vol.17 (2002) p.1190

Key Engineering Materials Vols. 309-311 (May 2006) pp. 263-266
online at http://www.scientific.net
© 2006 Trans Tech Publications, Switzerland

Cytotoxicity of Various Calcium Phosphate Ceramics

Masato Tamai[1a], Ryusuke Nakaoka[1b] and Toshie Tsuchiya[1c]
Division of Medical Devices, National Institute of Health Science
1-18-1 Kamiyoga, Setagaya-ku, Tokyo 158-8501 Japan
[a]m-tamai@nihs.go.jp, [b]nakaoka@nihs.go.jp, [c]tsuchiya@nihs.go.jp

Keywords: Calcium phosphate ceramics, Cytotoxicity,

Abstract. The cytotoxicity of five calcium phosphate ceramics, hydroxyapatite (HAp), flouroapatite (FAp), α-tricalcium phosphate (α-TCP), β-tricalcium phosphate (β-TCP) and tetracalcium phosphate (TTCP), was investigated. Based on the guidelines of biological test for medical devices in Japan, a cytotoxicity test of these calcium phosphates was carried out using Chinese hamster V79 lung fibroblasts. The cytotoxic study revealed that FAp and α-TCP showed high cytotoxicities. From various analyses, it was considered that the cytotoxicity of the FAp was due to fluorine ions extracted in a culture medium and the cytotoxicity of α-TCP resulted from a decrease in pH of the medium by the phosphoric acid, which produced by hydrolysis of the α-TCP.

Introduction

From the view point of biological affinity to bone, calcium phosphate (CP) ceramics have been studied to utilize for many purposes in a medical field. For instance, hydroxyapatite ($Ca_{10}(PO_4)_6(OH)_2$, HAp) and β-tricalcium phosphate (β-$Ca_3(PO_4)_2$, ß-TCP), are known to be biologically bonded to natural bones and their porous materials have been studied for effective restoration of bone defects.[1,2] Fluoroapatite ($Ca_{10}(PO_4)_6F_2$, FAp) has been reported to have a potential of novel bone repairing materials with high stability *in vivo*, since solubility of FAp is lower than that of HAp.[3,4] In addition, CP cement is also promising for bone repair and it is well known that α-tricalcium phosphate (α-$Ca_3(PO_4)_2$, α-TCP) and tetracalcium phosphate ($Ca_4(PO_4)_2O$, TTCP) are starting materials for the harden reaction of the bone cement.[5,6]

To develop biomaterials for utilizing for bone tissue, various properties, e.g. biological, physical and chemical property, should be satisfied. Among them, biological safety is important for the biomaterials. Since only a few studies which discuss the cytotoxicity of calcium phosphate ceramics have been reported, the cytotoxicity of CP ceramics is worthy to be investigated in order to design bioceramics with good biological safety for medical application. Therefore, the cytotoxicities of five calcium phosphate ceramics, hydroxyapatite (HAp), flouroapatite (FAp), α-tricalcium phosphate (α-TCP), β-tricalcium phosphate (β-TCP) and tetracalcium phosphate (TTCP) were investigated.

Materials and Methods

Materials

Five kinds of CP ceramics, HAp, FAp, α-TCP, β-TCP and TTCP were purchased from Wako chem. Co. Ltd. CP powders (0.25 g) was put into stainless mold and uniaxially pressed at 30MPa for 1 min to form a pellet. The dimensions of the obtained CP pellet were 1mm in thickness and 12mm in diameter. CP pellets were sterilized by an autoclave at 121°C for 20 min.

Cytotoxicty test on CP ceramics

Cytotoxicity test was carried out using Chinese hamster V79 lung fibroblasts by a colony assay system. V79 cells were maintained in Eagle's minimum essential medium (Nissui Pharmaceutical Co. Ltd.) with 10% fetal calf serum (FCS, Intergen Co. Ltd.) and incubated at 37 °C in a humidified atmosphere with 5% CO_2.

The method of cell seeding in the cytotoxicity test of CP ceramics was shown below; each CP pellets were placed in each culture wells of 24 well culture plates (Corning Co. Ltd.) and 300μl of culture medium was added into each well. Then, 50 cells/300μl of the cell suspension in the

culture medium were added into each well and incubated at 37°C for 4 h. Finally, 400μl of the culture medium was added into each well and the plates were incubated at 37 °C in a humidified atmosphere with 5 % CO_2 for 7days. In order to investigate a cell adhesive property on the CP ceramics, the culture medium was changed after 4 h and further incubated for 7days. The removed culture medium was transferred to another well of a new plate and incubated for 7days as well.

Cytotoxicity of extracts from CP ceramics was also investigated in this study. Suspensions of CP ceramics in the culture medium (100mg/mL) were stirred at 37°C for 3days under the rotation condition at 150rpm. The suspensions were centrifuged and the supernatants were collected as test extracts. In addition, media with various pH values were prepared using HCl solution to investigate an effect of pH on cell survival. Fifty V79 cells in 1ml of the extracts or the medium with different pH value were incubated at 37 °C for 7days.

After 7-day incubation, the cells were fixed in methanol and the number of the V79 colonies was counted after staining cells with 5%-Giemsa solution to estimate the cytotoxicity of the test sample. In addition, the pH of the medium after 7-days culture was measured to estimate the effect of the pH of the medium on the cytotoxicity test.

Characterization of CP ceramics

The structural changes of CP before and after an autoclave-sterilization or an incubation at 37°C culture were investigated by powder X-ray diffraction (XRD) analysis and scanning electron microscopy (SEM). XRD analysis was carried out (Rigaku Co., Ltd. / RINT 2000) with the CuK_α radiation at 40kV, 50mA. SEM observations were performed (JEOL / JSM-5800LV) with an accelerating voltage of 25kV.

Results and Discussion

Cytotoxicity of various CP ceramics

From XRD analysis, no structural changes of CPs were observed after an autoclave sterilization. After staining CP pellets, it was observed that cell colonies were formed on various CP ceramics pellets (Fig.1(a)). The results of the cytotoxicity test of CPs are shown in Fig.1(b). The cell colonies were hardly formed on FAp and α-TCP pellets and the ratios of the colonies formed on these pellets against V79-alone culture were 22.6% and 0.0%, respectively. In addition, the ratios of the colonies on the HAp, β-TCP and TTCP pellets were 58.1%, 57.3% and 78.4%, respectively. As no colonies were observed after 7-day culture of the removed medium in cell adhesion studies of CP ceramics, these results suggested that V79 cells can adhere and be viable on these pellets, irrespective of the type of CP ceramics. Figure 2 shows the formation of colonies cultured in extract from CP ceramics. The cytotoxicity test of extracts from CPs revealed that the tendency of their cytotoxicities was similar to that of the cytotoxicities on the respective CP pellets themselves (Fig.1(b)).

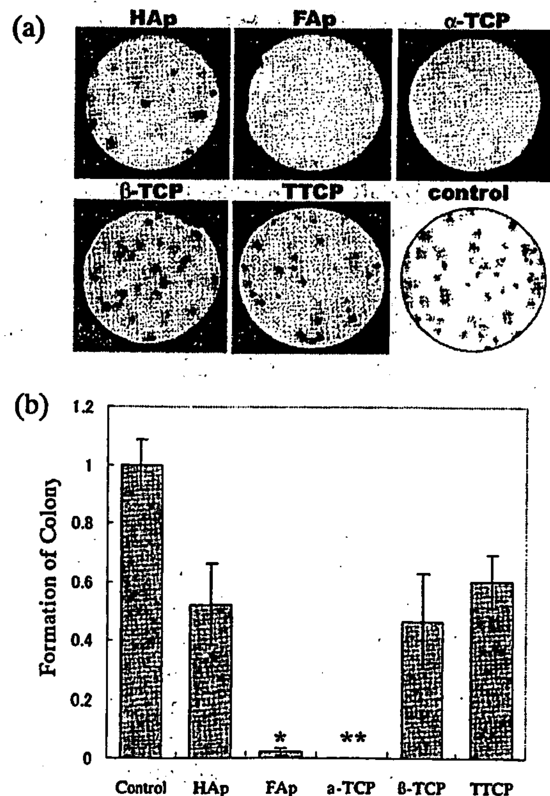

Fig.1. The appearance of colonies on various CP pellets (a) and their colony formation ratios (b). (*$p<0.05$ against for V79 alone, **$p<0.01$ against for V79 alone)